

1 Autumn – winter minimum temperature changes in the 2 southern Sikhote-Alin mountain range of northeast Asia since 3 1529 AD

4 Olga N. Ukhvatkina, Alexander M. Omelko, Alexander A. Zhmerenetsky, Tatyana Y. Petrenko.
5
6 Federal Scientific center of the East Asia terrestrial biodiversity Far Eastern Branch of Russian
7 Academy of Sciences, Vladivostok 690022 RUSSIA

8
9 *Correspondence to:* Olga Ukhvatkina (ukhvatkina@gmail.com)
10

11 **Abstract.** The aim of our research was to reconstruct climatic parameters (for the first time for the Sikhote-Alin
12 mountain range) and to compare them with global climate fluctuations. As a result, we have found that one of the
13 most important limiting factors for the study area is the minimum temperatures of the previous autumn-winter
14 season (August-December), and this finding perfectly conforms to that in other territories. We reconstructed the
15 previous August-December minimum temperature for 485 years, from 1529 to 2014. We found twelve cold periods
16 (1538-1543, 1549-1554, 1643-1649, 1659-1667, 1675-1689, 1722-1735, 1791-1803, 1807-1818, 1822-1827, 1836-
17 1852, 1868-1887, 1911-1925) and seven warm periods (1561-1584, 1603-1607, 1614-1618, 1738-1743, 1756-1759,
18 1776-1781, 1944-2014). These periods correlate well with reconstructed data for the Northern Hemisphere and the
19 neighboring territories of China and Japan. Our reconstruction has 2-4, 9-11, 48 and 189-year periods, which are in
20 line with high-frequency fluctuations in ENSO, the short-term solar cycle, PDO fluctuations and the de-Vier quazi-
21 200 solar activity cycle, respectively. We have confirmed the climatic response to solar activity, which corresponds
22 to cold periods during the solar minimum. These comparisons show that our climatic reconstruction based on tree-
23 ring chronology for this area may potentially provide a proxy record for long-term, large-scale past temperature
24 patterns for northeast Asia. The reconstruction reflects the global traits and local variations in the climatic processes
25 of the southern territory of the Russian Far East for more than the past 450 years.

26 1 Introduction

27 Global climate change is the main challenge for human life and natural systems, which is why we should clearly
28 understand climatic changes and their mechanisms. A retrospective review of climatic events is necessary for
29 understanding the climatic conditions from a long-term perspective. At the same time, instrumental climate
30 observations rarely cover more than a 100-year period and are often restricted to 50-70 years. This restriction forces
31 the researchers to continuously find new ways and methods to reconstruct climatic fluctuations. Dendrochronology
32 has been widely applied in climatic reconstruction for local territories and at the global scale for both climatic
33 reconstructions of the past few centuries and paleoclimatic reconstructions because it is rather precise, extensively
34 used and a replicable instrument (Corona et al.; Popa and Bouriaund, 2014; Kress et al., 2014; Lyu et al., 2016).
35 A great number of studies have focused on climatic change reconstruction for the northeastern parts of China based
36 on *P. koraeinsis* radial growth studies (e.g., Zhu et al., 2009; Wang et al., 2013; Wang et al., 2016; Zhu et al., 2015;
37 Lyu et al. 2016). Climatic parameters were reconstructed for the whole Northern Hemisphere (Wilson et al., 2016),
38 China (Ge et al., 2016), and temperature characteristics were reconstructed for northeastern Asia (Ohyama et al.,
39 2013). Despite this, there are very few studies of Russian Far East climate (e.g., Willes et al., 2014; Jacoby et al.,
40 2004; Shan et al., 2015); moreover, there is an absence of dendrochronological studies for the continental part of
41 Russian Far East. Meanwhile, most of species present in northeastern China, the Korean peninsula and Japan grow in

42 this region. In addition, the [distribution areas](#) of these trees often end in the south of the Russian Far East, which
43 increases the climatic sensitivity of plants. Additionally, some parts of the forests in the Russian Far Eastern have not
44 been subjected to human activity for the last 2000-4000 years. This makes it possible to forests extend the studied
45 timespan. In addition, the southern territory of the Russian Far East is sensitive to global climatic changes as it is
46 under the influence of cold air flow from northeastern Asia during the winter and summer monsoons. All of the factors
47 listed above create favorable conditions for dendroclimatic studies.

48 It is well-known that warming of the climate is correlated with intensive solar activity (e.g., the Medieval Warm
49 Period), while decreases in temperature occurs during periods of low solar activity (e.g., the Little Ice Age; Lean and
50 Rind, 1999; Bond et al., 2001). According to findings from an area of China neighboring the territory studied here,
51 the registered warming has been significantly affected by global warming since the 20th century (Ding and Dai, 1994;
52 Wang et al., 2004; Zhao et al., 2009), which is often indicated by a faster rise in night or minimum temperatures (Karl
53 et al., 1993; Ren and Zhai, 1998; Tang et al., 2005). To better understand and evaluate future temperature change
54 trends, we should study the long-term history of climatic changes.

55 However, using tree-ring series for northeastern Asia (particularly temperature) is rather complicated due to the unique
56 hydrothermal conditions of the region. Most reconstructions cover periods of less than 250 years (e.g., Shao and Wu,
57 1997; Zhu et al., 2009; Wang et al., 2012; Li and Wang, 2013; Yin et al., 2009; Zhu et al., 2015), except for a few
58 with periods up to 400 years (Lyu et al., 2016; Wiles et al., 2014). The short period of reconstructions is the reason
59 why such reconstructions cannot capture low-frequency climate variations.

60 The warming of the climate (particularly minimum temperature increase) is registered across the whole territory of
61 northeastern Asia (Lyu et al., 2016). In the Russian Far-East, such warming has been recorded for more than 40 past
62 years (Kozhevnikova, 2009). However, the lack of detailed climatic reconstructions for the last few centuries makes
63 it difficult to capture long-period climatic events for this territory and interpret the temperature conditions for the last
64 500-1000 years.

65 Therefore, the main objectives of this study were (1) to develop the first [three-ring-width chronology for the southern](#)
66 [part of the Russian Far East; \(2\) to analyze the regime of temperature variation over the past centuries in the southern](#)
67 [part of the Russian Far East; \(3\) to identify the recent warming amplitude in context of long-term changes and to](#)
68 [analyze the periodicity of climatic events and their driving forces.](#) Our new minimum temperature record supplements
69 the existing data for northeast Asia and provides new evidence of past climate variability. There is the potential to
70 better understand future climatic trajectories from these data in northeast Asia.

72 2 Materials and methods

73 2.1 Study area

74 We studied the western macroslope of the southern part of the Sikhote-Alin mountain range (Southeastern Russia) at
75 the Verkhneussuriysky Research Station of the Federal Scientific Center of the East Asia terrestrial biodiversity Far
76 East Branch of the Russian Academy of Sciences (4400 ha; N 44°01'35.3'', E 134°12'59.8'', Fig. 1).

77 The territory is characterized by a monsoon climate with relatively long, cold winters and warm, rainy summers. The
78 average annual air temperature is 0.9 °C; January is the coldest month (−32 °C average temperature), and July is the
79 warmest month (27 °C average temperature). The average annual precipitation is 832 mm (Kozhevnikova, 2009).
80 Southerly and southeasterly winds predominate during the spring and summer, while northerly and northwesterly
81 winds predominate in autumn and winter. The terrain includes mountain slopes with an average angle of ~ 20°, and
82 the study area is characterized by brown mountain forest soils (Ivanov, 1964) (Fig. 2).

83 Mixed forests with Korean pine (*Pinus koraiensis* Siebold et Zucc.) are the main vegetation type in the study area,
84 and they form an altitudinal belt up to 800 m above sea level. These trees are gradually replaced by coniferous fir-
85 spruce forests at high altitudes (Kolesnikov, 1956). Korean pine-broadleaved forests are formed by up to 30 tree
86 species, with *Abies nephrolepis* (Trautv.) Maxim, *Betula costata* (Trautv.) Regel., *Picea jezoensis* (Siebold et Zucc.)
87 Carr., *P. koraiensis* and *Tilia amurensis* Rupr. being dominant.

88 Korean pine-broadleaved forests are the main forest vegetation type in the Sikhote-Alin mountain range in the
89 southern part of the Russian Far East. This area is the northeastern limit of the range of Korean pine-broadleaved
90 forests, which are also found in northeastern China (the central part of the range), on the Korean peninsula, and in
91 Japan. The Sikhote-Alin mountain range is one of the few places where significant areas of old-growth Korean pine-
92 broadleaved forest remain. In the absence of volcanic activity, which is a source of strong natural disturbances in the
93 central part of the range (Liu, 1997; Ishikava, 1999; Dai et al., 2011), wind is the primary disturbance factor on this
94 territory. Wind causes a wide range of disturbance events, from individual treefalls to large blowdowns (Dai et al.,
95 2011).

96 Approximately 60% of the Research Station area had been subjected to selective clear-cutting before the station was
97 established in 1972. The remaining 40% of its area has never been clear-cut and is covered by unique old-growth
98 forest.

99 2.2 Tree-ring chronology development

100 Our study is based on data collected in a 10.5-ha permanent plot (Omelko and Ukhvatkina, 2012; Omelko et al., 2016),
101 which was located in the middle portion of a west-facing slope with an angle of 22° at a gradient altitude 750-950 m
102 above sea level. The forest in the plot was a late-successional stand belonging to the middle type of Korean pine-
103 broadleaved forests at the upper bound of the distribution of Korean pine, where it forms mixed stands of Korean
104 pine-spruce and spruce-broadleaved forests (Kolesnikov, 1956).

105 One core per undamaged old-growth mature tree (25 cores from 25 trees) and one sample from dead trees (20 samples)
106 were extracted from *P. koraiensis* trees in the sample plots from the trunks at breast height. In the laboratory, all tree-
107 ring samples were mounted, dried and progressively sanded to a fine polish until individual tracheids within annual
108 rings were visible under an anatomical microscope according to standard dendrochronological procedures (Fritts,
109 1976; Cook and Kairiukstis, 1990). Preliminary calendar years were assigned to each growth ring, and possible errors
110 in measurement due to false or locally absent rings were identified using the Skeleton-plot cross-dating method
111 (Stokes and Smiley, 1968). The cores were measured using the semi-automatic Velmex measuring system (Velmex,
112 Inc., Bloomfield, NY, USA) with a precision of 0.01 mm. Then, the COFECHA program was used to check the
113 accuracy of the cross-dated measurements (Holmes, 1983). To mitigate the potential trend distortion problem in
114 traditionally detrended chronology (Melvin and Briffa, 2008; Anchukaitis et al., 2013), we used a signal-free method
115 (Melvin and Briffa, 2008) to detrend the tree-ring series using the RCSigFree program (<http://www.ldeo.columbia.edu/tree-ring-laboratory/resources/software>).

117 Age-related trends were removed from the raw tree-ring series using an age-dependent spline smoothing method. The
118 ratio method was used to calculate tree-ring indices, and the age-dependent spline was selected to stabilize the variance
119 caused by core numbers. Finally, the stabilized signal-free chronology was used for the subsequent analysis (Fig. 3).
120 The mean correlations between trees (*R*_{bt}), mean sensitivity (MS) and expressed population signal (EPS) were
121 calculated to evaluate the quality of the chronology (Fritts, 1976). *R*_{bt} reflects the high-frequency variance, and MS
122 describes the mean percentage change from each measured annual ring value to the next (Fritts, 1976; Cook and
123 Kairiukstis, 1990). EPS indicates the extent to which the sample size is representative of a theoretical population with

124 an infinite number of individuals. A level of 0.85 in the EPS is considered to indicate a chronology of satisfactory
125 quality (Wigley *et al.*, 1984). The statistical characteristics of the chronology are listed in Table 1.
126 The full length of the chronology spans (VUS chronology) from 1451 to 2015. A generally acceptable threshold of
127 the EPS was consistently greater than 0.85 from AD 1602 to 2015 (9 trees; Fig. 3b), which affirmed that this is a
128 reliable period. However, although the EPS value from AD 1529 to 1602 was less than 0.85, it matches a minimum
129 sample depth of 4 trees in this segment (EPS>0.75). It is very important to extend the tree-ring chronology as much
130 as possible because there are only a few long climate reconstructions in this area. Therefore, we retained the part from
131 1529 to 1602 in the reconstruction.

132 2.3 Climate data and statistical methods

133 Monthly precipitation, monthly mean and minimum temperature data were obtained from the Chuguevka
134 meteorological station (44.151462 N, 133.869530 E) and the meteorological post at the Verkhneussuriisky research
135 station of the Federal Scientific Center of the East Asia terrestrial biodiversity FEB RAS (Meteostation 7 – MP7) as
136 well. The periods of monthly data available from the Chuguevka and Verkhneussuriisky stations are 1936-2004 and
137 1969-2004, respectively (1971-2003 for minimum temperature data from the Chuguevka).

138 To demonstrate that our reconstruction representative and reflect temperature variations, we conducted spatial
139 correlation between our temperature reconstruction and gridded temperature dataset of the Climate Research Unit
140 (CRU TS4.00) for the period 1960-2003, by using the Royal Netherlands Meteorological Institute climate explorer
141 (<http://climexp.knmi.nl>).
142

143 2.4 Statistical analyses

144 A correlation analysis was used to evaluate the relationships between the ring-width index and observed monthly
145 climate records from the previous June to the current September. To identify the climate-growth relationships of
146 Korean pine in the southern Sikhote-Alin mountain range, a Pearson's correlation was performed between climate
147 variables and tree-width index. We used a traditional split-period calibration/verification method to explore the
148 temporal stability and reliability of the reconstruction model (Fritts, 1976; Cook and Kairiukstis, 1990). The Pearson's
149 correlation coefficient (r), R-squared (R^2), the reduction of the error (RE) the coefficient of efficiency (CE), and the
150 product means test (PMT) were used to verify the results. Analyses were carried out in R using the treeclim package
151 (Zang and Biondi, 2015) and STATISTICA software (StatSoft®).

152 3 Results

153 3.1 Climate-radial growth relationship

154 Relationships between the VUS chronology and monthly climate data are shown in Fig. 4. To reveal the correlation
155 between climatic parameters and radial growth change of *P. koraiensis*, we had three data sets: the first-time series
156 had a length of 68 years (1936-2004, Chuguevka), the second had a length of 34 years (1966-2000, MP7), and the
157 third had a length of 33 years (1971-2003, Chuguevka, minimum temperature). To select the appropriate parameters,
158 we analyzed all datasets. As a result, we revealed a reliable but slight positive correlation between *P. koraiensis* growth
159 and precipitation in May and June of the current year and September of the previous year in the territory of Chuguevka
160 village (Fig. 4a). There is also a slight positive correlation with precipitation in September of the previous year and

161 May of the current year at Metheostation 7 (MP7) (Fig. 4b). In addition, we revealed a slight negative correlation with
162 precipitation in February-March of the current year.

163 As for the correlation between temperature and *P. koraiensis* growth, the analysis reveals a weak positive correlation
164 with the average monthly temperature in June of the previous year and in February-April of the current year in the
165 Chuguevka settlement and a slight negative correlation with the average monthly temperature in June-July as well
166 (Fig. 4c). The analysis of the correlation with the average monthly temperature at Metheostation 7 (MP7) shows us a
167 weak positive correlation with temperature in August and December of the preceding year and a negative correlation
168 with temperature in July of the current year (Fig. 4d). In addition, we analyzed the correlation with minimum average
169 monthly temperatures at MP7 and Chuguevka. The revealed correlation with minimum temperature is reliable but
170 weak (Fig. 4e,f).

171 Moreover, based on the weak interaction that was revealed, we analyzed the correlation with climatic parameters for
172 selected ranges of months (Fig. 4h,g). The most stable correlation appears between growth and the minimum monthly
173 temperature of August-December of the previous year at Chuguevka (Fig. 4h), on which we base our subsequent
174 reconstructions.

175 3.2 Minimum temperature reconstruction

176 Basing on analysis of the correlation between climatic parameters and Korean pine growth, we constructed a linear
177 regression equation to reconstruct the minimum monthly temperature of August-December of the previous year
178 (VUSr). The transfer function was as follows:

$$179 \text{VUSr} = 7.189X_t - 15.161$$

$$180 (N=32, R=0.620, R^2=0.385, R^2_{\text{adj}}=0.364, F=18.76, p < 0.001)$$

181 where VUSr is the August-December minimum temperature at Chuguevka and X is the tree-ring index of the Korean
182 pine RSC chronology in year t . The comparison between the reconstructed and observed mean growing season
183 temperatures during the calibration period is shown in Fig. 5(a). The cross-validation test for the calibration period
184 (1971-1997, $R=0.624$) yielded a positive RE of 0.334, a CE of 0.284, and the cross-validation test for calibration
185 period 1977-2003 ($R=0.542$) a positive RE of 0.654, a CE of 0.644, confirming the predictive ability of the model.

186 Although during the study period, the model shows the observed values very well, the short observation period (1971-
187 2003) does not allow using split-sampling calibration and verification methods in full for evaluating quality and model
188 stability. This limitation is why we used a bootstrapping resampling approach (Efron, 1979; Young, 1994) for stability
189 evaluation and transfer function precision. The idea that this method is based on indicates that the available data
190 already include all the necessary information for describing the empirical probability for all statistics of interest.
191 Bootstrapping can provide the standard errors of statistical estimators even when no theory exists (Lui et al., 2009).
192 The calibration and verification statistics are shown in Table 2. The statistical parameters used in bootstrapping are
193 very similar to those from the original regression model, and this proves that the model is quite stable and reliable and
194 that it can be used for temperature reconstruction.

195

196 3.3 Temperature variations from AD 1529 to 2014 and temperature periodicity

197 Variations in the reconstructed average minimum temperature of the previous August-December (VUSr) since AD
198 1529 and its 21-year moving average are shown in Fig. 5b. The 21-year moving average of the reconstructed series
199 was used to obtain low-frequency information and analyze temperature variability in this region. The mean value of

200 the 486-year reconstructed temperature was -7.93°C with a standard deviation of $\pm 1.40^{\circ}\text{C}$. We defined warm and
201 cold periods as when temperature deviated from the mean value plus or minus 0.5 times the standard deviation,
202 respectively (Fig. 5b).

203 Hence, warm periods occurred in 1561-1584, 1603-1607, 1614-1618, 1738-1743, 1756-1759, 1776-1781, 1944-2014,
204 and cold periods appeared in 1538-1543, 1549-1554, 1643-1649, 1659-1667, 1675-1689, 1722-1735, 1791-1803,
205 1807-1818, 1822-1827, 1836-1852, 1868-1887, 1911-1925. Among them, the four warmest years were in 1574 ($-$
206 4.35°C), 1606 (-5.35°C), 1615 (-5.71°C), 1741 (-5.36°C), 1757 (-6.16°C), 1779 (-5.21°C), 2008 (-2.72°C), while
207 the three coldest year were in 1543 (-9.84°C), 1551 (-9.88°C), 1647 (-10.77°C), 1662 (-11.10°C), 1685 (-9.45°C),
208 1728 (-10.08°C), 1799 (-10.70°C), 1815 (-10.13°C), 1825 (-9.87°C), 1843 (-10.55°C), 1883 (-10.73°C), 1913 ($-$
209 10.29°C). The longest cold period extended from 1868 to 1887, and the longest warm period extended from 1944 to
210 present day. The coldest year is 1662 (-11.10°C) and the warmest year is 2008 (-2.72°C).

211 The MTM spectral analysis over the full length of our reconstruction revealed significant ($p < 0.05$) cycle peaks at
212 2.3-year (95%), 2.5-year (99%), 2.9-year (99%), 3.0-year (99%), 3.3-year (95%), 3.7-year (95%), 8.9-year (99%)
213 short periods and 20.4-year (95%), 47.6-year (95%), 188.7-year (99%) long periods (Fig. 6).

214 Spatial correlations between our reconstruction and the CRU TS4.00 temperature dataset reveal our record's
215 geographical representation (Fig. 7). The results show that the reconstruction of mean minimum temperature of
216 previous August – December is significantly positively correlated with the CRU TS4.00 ($r=0.568$, $p<0.0001$).

217 4 Discussion

218 4.1 Climate-growth relationships

219 The results of our analysis suggest that the radial growth of Korean pine in the southern part of the Sikhote-Alin
220 mountain range is mainly limited by the pre-growth autumn-winter season temperatures, in particular the minimum
221 temperatures of August-December (Fig. 4). It is widely known that tree-ring growth in cold and wet ecotopes, situated
222 on sufficiently high elevation in the Northern Hemisphere, strongly correlate with temperature variability in large
223 areas of Asia, Eurasia, North America (Zhu et al., 2009; Anchukaitis et al., 2013; Thapa et al., 2015; Wiles et al.,
224 2014). The limiting influence of temperature on *P. koraiensis* growth has been mentioned in many studies (Wang et
225 al., 2016; Yin et al., 2009; Wang et al., 2013; Zhu et al., 2009). However, the temperature has various limiting effects
226 in different conditions, and these limiting effects manifest in different ways (Wang et al., 2016). For example, Zhu et
227 al., 2016 indicates that in more northern and arid conditions of the Zhanguangcai Mountains, while precipitation is
228 not the main limiting factor, precipitation is considerably below evaporation during the growth season. This finding
229 is why a stable correlation between *P. koraiensis* growth and the growth season temperature is revealed. This finding
230 is also why moisture availability in soil might be the main limiting factor for Korean pine growth (Zhu et al., 2016),
231 but the emergence of this circumstance can be different in different conditions.

232 The correlation between growth and minimum temperatures in August-December of the previous year, as revealed
233 in our research, was also mentioned for Korean pine in other works (Wang et al., 2016; Zhu et al., 2009). This
234 finding may be explained by the following circumstances. Extreme temperatures limit the growth of trees at the tree
235 line or in high-latitude forests (Wilson and Luckman, 2002; Körner and Paulsen, 2004; Porter et al., 2013; Yin et al.,
236 2015). Taking into consideration the fact that the study area is situated at the altitudinal limit of Korean pine forest
237 distributions, in particular the Korean pine (Kolesnikov, 1956), these findings seem to be reliable.

238 In addition, in the conditions close to extreme for this species, low temperatures in autumn-winter may lead to thicker
239 snow cover, which melts far more slowly in spring (Zhang et al., 2015). The study area is notable for its dry spring,
240 and the amount of precipitation is minimal during the most important period of tree-growth in April-May
241 (Kozhevnikova, 2009). If the vegetation period of the plant cannot begin at the end of March and packed snow cover
242 melting is impeded up until the beginning of May, plant growth may be reduced. Moreover, although cambial activity
243 stops in the winter, organic components are still synthesized by photosynthesis. Low temperatures (in the territory of
244 the VUSr it can reach -48°C in certain years) may induce to loss of accumulated materials, which adversely affects
245 growth (Zhang et al., 2015). The study area is in the center of the vegetated area, where the conditions for Korean
246 pine growth are optimal during the growing season, and only minimum temperature is regarded as an extreme factor.

247 4.2 Comparison with other tree-ring-based temperature reconstructions

248 At present, temperature reconstructions are uncommon for the Russian Far East, and research sites are located for
249 thousands of kilometers away from one another. For example, Wiles et al. undertook a study of summer temperatures
250 on Sakhalin Island (Wiles et al., 2014). Unfortunately, it is impossible to compare our findings with theirs because
251 Sakhalin Island is climatically far more similar to Japanese islands than to the Sikhote-Alin mountains, and
252 temperature variations in their study area are mainly caused by oceanic currents.

253 In addition, instrumental observations from the study area rarely encompass a period longer than 50 years (and studies
254 have only been conducted for large settlements). Consequently, the tree-ring record serves as a good indicator of the
255 past cold-warm fluctuations in the Russian Far East. The analysis of spatial correlations between our reconstruction
256 and the CRU TS4.00 temperature dataset reveal spatial correlations between the observed and reconstruction
257 minimum temperatures from the CRU TS4.00 gridded T_{\min} dataset during the baseline period of 1960-2003 (Fig. 7).
258 It's indicating that our temperature reconstruction is representative of large-scale regional temperature variations and
259 can be taken as representative of southeastern of the Russian Far East and northeastern of the China.

260 To identify the regional representativeness of our reconstruction, we compared it with two temperature reconstructions
261 for surroundings areas and a reconstruction for the Northern Hemisphere (Fig. 8). The first reconstruction was for
262 summer temperatures in the Northern Hemisphere (Wilson et al., 2016). The second reconstruction was an April-July
263 tree-ring-based minimum temperature reconstruction for Laobai Mountain (northeast China), which is approximately
264 500 km northwest of our site. The third was a February-April temperature reconstruction for the Changbai Mountains
265 (Zhu et al., 2009), which are approximately 430 km southwest of our site.

266 Cold and warm periods are shown in table 3 (the duration is given by the authors of the article). The reconstructions
267 show that practically all cold and warm periods coincide but have different durations and intensities. The data on
268 Northern Hemisphere show considerable overlaps of cold and warm periods, and the correlation between
269 reconstructions is 0.45 ($p > 0.001$). At the same time, we found the warm period 1561-1584, which is not clearly
270 shown in reconstruction for the Northern Hemisphere, though the general trend of temperature change is maintained
271 during this period (Fig. 8). Long cold periods from 1643 to 1667 and 1675-1690 that were revealed for another territory
272 (Lyu et al., 2016; Wilson et al., 2016) coincided with the Maunder Minimum (1645–1715), an interval of decreased
273 solar irradiance (Bard et al., 2000). The coldest year in this study (1662) revealed in this period too. The Dalton
274 minimum period centered in 1810 is also notable. Interestingly that cold periods of 1807-1818, 1822-1827, 1836-1852
275 and 1868-1887 is also registered in reconstructions for Asia (Ohayama et al., 2013) and by Japanese researchers
276 (Fukaishi & Tagami, 1992; Hirano & Mikami, 2007). Moreover, instrumental observations reconstructed for western
277 Japanese territories (the nearest to the study area) provide evidence of a cold period in the 1830s-1880s with a short
278 warm spell in the 1850s (Zaiki et al., 2006), which is in agreement with our data (not reliably period 1855-1865, Tabl.

279 3). For this period, there are contemporaneous records of severe hunger in Japan in 1832 and 1839, which was the
280 result of a summer temperature decrease and rice crop failure (Nishimura & Yoshikawa, 1936).
281 In this case, the longer cold period for the study area can be explained by the relatively lower influence of the warm
282 current and monsoon and generally colder climate in the south of the Russian Far East compared with Japanese islands.
283 The differing opinion about the three cold periods in China in the 17th, 18th and 19th centuries (Wang et al., 2003) is
284 also corroborated by our reconstruction. The cold period in the 19th century is even more pronounced than that reported
285 by Lyu et al., 2016. Moreover, Lyu et al., 2016 corroborate that the ascertained cold period in 19th century is more
286 evident in South China, but it is less clear in the northern territories or has inverse trend. Although the Russian Far
287 East is further north than the southern Chinese provinces and is closer to the northern part of the country, the marked
288 monsoon climate likely made it possible to reflect the general cold trend in 19th century, which was typical both for
289 China and the entire Northern Hemisphere. Because of this possible explanation, the cold period in the 19th century
290 for the Changbai Mountains shows up more distinctly than for the northern and western territory of Laobai Mountain
291 (Fig. 8).
292 Apparently, this discrepancy in regional climate flow is the reason that our reconstruction agrees well with the general
293 reconstruction for the whole hemisphere ($r = 0.45, p < 0.001$) and to a lesser extent agrees with the regional curves for
294 Laobai Mountain ($r = 0.23, p < 0.001$) and Changbai Mountain ($r = 0.32, p < 0.001$).
295 The changing dynamics of the 20th century temperature are also interesting to watch. **The comparison of the minimum
296 annual temperatures for the territory and the reconstructed data for the period of 1960-2003 shows significant data
297 correlation (Fig. 7), including the northeast part of China.** At the same time, for Chinese territory (both for southwest
298 regions and for more northwestern regions), the warming is apparent only in the last quarter century (Zhu et al., 2009)
299 or at the end of the 20th century (Lyu et al., 2016) (Fig. 8 c,d). This trend, revealed for the southern Sikhote-Alin
300 mountains (a warm spell since 1944), is corroborated for the whole Northern Hemisphere (Wison et al., 2016) (Fig.
301 8a,b). The maximum cold period is also corroborated, which we note for the 19th century (Fig. 8a,b).
302 The probable explanation is in the regional climate flow differences in the compared data. The territory of northeastern
303 China is more continental, though the influence of the Pacific Ocean is also notable. At the same time, the southern
304 part of the Sikhote-Alin mountains is more prone to the influence of monsoons, as are the Japanese islands. According
305 to paleoreconstructions, the Little Ice Age occurred in the Northern Hemisphere 600-150 years ago (Borisova, 2014).
306 The period of landscape formation for the Sikhote-Alin range during the transition from the Little Ice Age to
307 contemporary conditions occurred within the last 230 years (Razzhigaeva et al., 2016). The timeframe of the Little
308 Ice Age is generally recognized as varying considerably depending on the region (Bazarova et al., 2014). However, it
309 is certain that the Little Ice Age is accompanied by an increase in humidity in coastal areas of northeast Asia (Bazarova
310 et al., 2014). Thus, in similar conditions on the Japanese islands, the Little Ice Age was accompanied by lingering and
311 intensive rains (Sakaguchi, 1983), and the last typhoon activity was registered for the Japanese islands from the middle
312 of the 17th century to the end of the 19th century (Woodruff et al., 2009). At the same time, the reconstruction of
313 climatic changes for the whole territory of China for the last 2000 years (Ge et al., 2016) shows that the cold period
314 lasted until 1920, which correlates with the data we obtained. This timespan wholly coincides with our data, and we
315 can draw the conclusion that in the southern region of the Sikhote-Alin mountains, the Little Ice Age ended at the turn
316 of the 19th century.
317 Unfortunately, when comparing temperature, different changes were also observed for some cold and warm years
318 (Fig. 7). This finding may be attributed to differences in the reconstructed temperature parameters (such as average
319 value, minimum temperature and maximum temperature) and environmental conditions in different sampling regions.
320 Recent studies show that the oscillations in the medium, minimum and maximum temperature are often asymmetrical

321 (Karl et al., 1993; Xie and Cao, 1996; Wilson and Luckman, 2002, 2003; Gou et al., 2008). The global warming over
322 the past few decades has been mainly caused by the rapid growth of night or minimum temperatures but not maximum
323 temperatures. Meanwhile, some differences between the reconstructed temperature values were well explained by a
324 comparison with similar areas. So, for the first time, these results can characterize regional climate variations and
325 provide reliable data for large-scale reconstructions for the northeastern portion of Eurasia.

326 **4.3 Periodicity of climatic changes and their links to global climate processes**

327 Among the significant periodicities in the reconstructed temperature detected by the MTM analysis (Fig. 7), some
328 peaks were singled out: 2.3-year (95%), 2.5-year (99%), 2.9-year (99%), 3.0-year (99%), 3.3-year (95%), 3.7-year
329 (95%), 8.9-year (99%) short periods and 20.4-year (95%), 47.6-year (95%), and 188.7-year (99%) long periods.

330 The 2-4-year cycle may be linked with the El Niño-Southern Oscillation (ENSO). These high-frequency (2-7-year)
331 cycles (Bradley *et al.*, 1987) have also been found in other tree-ring-based temperature reconstructions in northeast
332 Asia (Zhu *et al.*, 2009; Li and Wang, 2013; Zhu et al., 2016; Gao et al., 2015).

333 The 2–3-year quasi-cycles may also correspond to the quasi-biennial oscillation (Labitzke and van Loon, 1999) and
334 the tropospheric biennial oscillation (Meehl, 1987), whereas the 8.9-11.5-year cycles may correspond to solar activity.
335 Considering the coincidence of these two episodes, the Maunder Minimum (1645–1715) and the Dalton minimum
336 period centered in 1810, the revealed periodicity seems reliable.

337 It seems that next low-frequency cycles of 20 and 48 years reflect processes influenced by Pacific Decadal Oscillation
338 (PDO, Mantua and Hare 2002) variability, which has been found at 15-25-yr and 50-70-yr cycles (Ma, 2007).

339 Given that many researchers working in the territory of northeast Asia have also revealed these cycles in relation to
340 the Korean pine, we can draw a conclusion that Korean pine tree-ring series support the concept of long-term,
341 multidecadal variations in the Pacific (e.g., D'Arrigo et al., 2001; Cook, 2002) and that such variation or shifts have
342 been present in the Pacific for several centuries.

343 Despite the fact that it is quite difficult to reveal for certain long-period cycles in a 486-year chronology, we
344 nonetheless revealed the 189-year cycle. Such periodicity is revealed in long-term climate reconstructions and is
345 linked to the quasi-200-year solar activity cycle (Raspopov et al., 2009). Such climate cycling, linked not only to
346 temperature but also to precipitation, is revealed for the territories of Asia, North America, Australia, Arctic and
347 Antarctic (Raspopov et al., 2008). At the same time, the 200-year cycle (*de-Vries* cycle) may often have a phase shift
348 from some years to decades and correlates not only positively but also negatively with climatic fluctuations depending
349 on the character of the nonlinear response of the atmosphere-ocean system within the scope of the region (Raspopov
350 et al., 2009). According to Raspopov et al. (2009), the study area is in the zone that reacts with a positive correlation
351 to solar activity, though the authors note that we should not expect a direct response because of the nonlinear character
352 of the atmosphere-ocean system reaction to variability in solar activity (Raspopov et al., 2009). Taking into
353 consideration this fact and that the cold and warm periods shown in our reconstruction are slightly shifted compared
354 with more continental areas and the whole Northern Hemisphere, we can say that the reconstruction of minimum
355 August-December temperatures reflects the global climate change process in aggregate with the regional
356 characteristics of the study area.

357 **Conclusions**

358 Using the tree-ring width of *Pinus koraiensis*, the mean minimum temperature of the previous August-December has
359 been reconstructed for the southern part of Sikhote-Alin Mountain Range, northeastern Asia, Russia, for the past 486

360 years. This dataset is the first climate reconstruction for this region, and for the first time for northeast Asia, we present
361 a reconstruction with a length exceeding 486 years.
362 Because explained variance of our reconstruction is about 39%, we believe that the result is noteworthy as it displays
363 the respective temperature fluctuations for the whole region, including northeast China, the Korean peninsula and the
364 Japanese archipelago. Our reconstruction is also in good agreement with the climatic reconstruction for the whole
365 Northern Hemisphere. The reconstruction shows good agreement with the cold periods described by documentary
366 notes in eastern China and Japan. All these comparisons prove that for this region, the climatic reconstruction based
367 on tree-ring chronology has a good potential to provide a proxy record for long-term, large-scale past temperature
368 patterns for northeast Asia. The results display the cold and warm periods in the region, which are conditional on
369 global climatic processes (PDO, ENSO), and reflect the influence of solar activity (we revealed the influence of the
370 11-year and 200-year solar activity cycles). At the same time, the reconstruction highlights the peculiarities of the
371 flows of global process in the study area and helps in understanding the processes in the southern territory of the
372 Russian Far East for more than the past 450 years. Undoubtedly, the results of our research are important for studying
373 the climatic processes that have occurred in the study region and in all of northeastern Asia and for situating them
374 within the scope of global climatic change.

375

376 **Acknowledgements** This work was funded by Russian Foundation for Basic Research, Project 15-04-02185.

377 **References**

- 378 Anchukaitis K.J., D'Arrigo R.D., Andreu-Hayles L., Frank D., Verstege A., Curtis A., Buckley B.M., Jacoby G.C.,
379 and Cook E.R.: Tree-ring-reconstructed summer temperatures from Northwestern North America during the last
380 nine centuries. *J Clim.* 26, 3001-3012, doi: 10.1175/JCLI-D-11-00139.1, 2013.
- 381 Bard E., Raisbeck G., Yiou F. and Jouzel J.: Solar irradiance during the last 1200 years based on cosmogenic
382 nuclides. *Tellus B.*, 52, 985-992, 2000.
- 383 Bazarova V.B., Grebennikova T.A., and Orlova L.A.: Natural-environment dynamic within the Amur basin during
384 the neoglacial. *Geogr. Nat. Resour.*, 35(3), 275-283, doi: 10.1134/S1875372814030111, 2014.
- 385 Bond G., Kromer B., Beer J., Muscheler R., Evans M.N., Showers W., Hoffmann S., Lotti-Bond R., Hajdas I.,
386 Bonani G.: Persistent solar influence on north Atlantic climate during the Holocene. *Sci.*, 294, 2130–2136, 2001.
- 387 Borisova O.K.: Landscape-climatic changes in Holocene. *Reg. Res. Rus.*, 2, 5-20, 2014.
- 388 Bradley R.S., Diaz H.F., Kiladis G.N., Eischeid J.K.: ENSO signal in continental temperature and precipitation
389 records. *Nat.* 327, 497-501, 1987.
- 390 Cook E.R., Kairiukstis L.A.: *Methods of dendrochronology: applications in the environmental sciences.* Kluwer
391 Academic Publishers, Dordrecht, 1990.
- 392 Cook E.R.: Reconstructions of Pacific decadal variability from long tree-ring records. *Eos Trans. 83 (19) Spring*
393 *Meet. Suppl.*, Abstract GC42A-04, 2002.
- 394 Corona C., Guiot J., Edouard J.L., Chalié F., Büntgen U., Nola P. and Urbinati C.: Millennium-long summer
395 temperature variations in the European Alps as reconstructed from tree rings. *Clim. Past.*, 6, 379-400,
396 doi:10.5194/cp-6-379-2010, 2012.
- 397 Dai L.M., Qi L., Su D.K., Wang Q.W., Ye Y.J. and Wang Y.: Changes in forest structure and composition on
398 Changbai Mountain in Northeast China. *Ann. For. Sci.*, 68, 889-897, 2011.
- 399 Ding Y., Dai X.: Temperature Variation in China during the Last 100 years. *Meteorology*, 20, 19-26, 1994.

400 Durbin J. and Watson G.S.: Testing for serial correlation in least squares regression. *Biometrika*, 38, 159-178, 1951.

401 Efron B.: The jackknife, the bootstrap, and other resampling plans. Pa. Soc. for Industrial and Appl. Mathem.,
402 Philadelphia, 1982.

403 Efron B.: Bootstrap methods: another look at the jackknife. *Annals Statistics*, 7, 1-26, 1979.

404 Fritts H.C.: Tree rings and climate. Academic Press Inc., London, 1976.

405 Fukaishi K. and Tagami Y.: An attempt of reconstructing the winter weather situations from 1720–1869 by the use
406 of historical documents. In: Proceedings of the International Symposium on the Little Ice Age Climate, Department
407 of Geography, Tokyo Metropolitan University, Tokyo, 194-201, 1992.

408 Ge Q., Zheng J., Hao Z., Liu Y. and Li M.: Recent advances on reconstruction of climate and extreme events in
409 China for the past 2000 years. *J Geogr Sci* 26(7), 827-854, doi: 10.1007/s11442-016-1301-4, 2016.

410 Gou X., Chen F., Yang M., Gordon J., Fang K., Tian Q. and Zhang Y.: Asymmetric variability between maximum
411 and minimum temperatures in Northeastern Tibetan Plateau: evidence from tree rings. *Sci. China. Ser. D*, 51, 41-55,
412 2008.

413 Hirano J. and Mikami T.: Reconstruction of winter climate variations during the 19th century in Japan. *Int J*
414 *Climatol* 28, 1423-1434, doi:10.1002/joc.1632, 2007.

415 Holmes R.L.: Computer-assisted quality control in tree-ring dating and measurement. *Tree-ring Bull.* 43, 69-78,
416 1983.

417 Ishikawa Y., Krestov P.V. and Namikawa K.: Disturbance history and tree establishment in old-growth *Pinus*
418 *koraensis*-hardwood forests in the Russian Far East. *J. Veg. Sci.* 10, 439-448, 1999.

419 Karl T.R., Jones P.D., Knight R.W., Kulas G., Plummer N., Razuvayev V., Gallo K.P., Lindsey J., Charlson R.J.,
420 and Peterson T.C.: A new perspective on recent global warming: asymmetric trends of daily maximum and
421 minimum temperature. *B. Am. Meteorol. Soc.*, 74, 1007-1023, 1993.

422 Kolesnikov B.P.: Korean pine forests of the [Russian] Far East. *Trudy DVF AN SSSR.* 2, 1-264, 1956 (In Russian).

423 Körner C. and Paulsen J.: A world-wide study of high altitude treeline temperatures. *J. Biogeogr.*, 31, 713-732,
424 doi:10.1111/j.1365-2699.2003.01043.x, 2004.

425 Kozhevnikova N.K.: Dynamics of weather-climatic characteristics and ecological function of small river basin. *Sib.*
426 *Ecol. J.*, 5, 93-703, 2009 (In Russian).

427 Kress A., Hangartner S., Bugmann H., Büntgen U., Frank D.C., Leuenberger M., Siegwolf R.T.W. and Saurer M.:
428 Swiss tree rings reveal warm and wet summers during medieval times. *Geophys. Res. Lett.*, 41, 1732-1737, doi:
429 10.1002/2013GL059081, 2014.

430 Labitzke K.G. and van Loon H.: *The Stratosphere: Phenomena, History and Relevance.* Springer, Berlin, 1999.

431 Lean J. and Rind D.: Evaluating sun-climate relationships since the Little Ice Age. *J. Atmos. Sol. Terr. Phys.*, 61,
432 25-36, 1999.

433 Li M. and Wang X.: Climate-growth relationships of three hard- wood species and Korean pine and minimum
434 temperature reconstruction in growing season in Dunhua, China. *J. Nanjing. For. Univ.*, 37, 29-34, 2013.

435 Liu Y., Bao G., Song H., Cai Q. and Sun J.: Precipitation reconstruction from Hailar pine (*Pinus koraiensis* var.
436 *mongolica*) tree rings in the Hailar region, Inner Mongolia, China back to 1865 AD. *Paleogeogr Paleoclimatol*
437 *Paleoecol.* 282, 81-87, doi:10.1016/j.palaeo.2009.08.012, 2009.

438 Liu Q.J.: Structure and dynamics of the subalpine coniferous forest on Changbai mountain, China. *Plant. Ecol.* 132,
439 97-105, 1997.

440 Lu R., Jia F., Gao S., Shang Y. and Chen Y.: Tree-ring reconstruction of January-March minimum temperatures
441 since 1804 on Hasi Mountain, northwestern China. *J. Arid. Environ.*, 127, 66-73,
442 doi:10.1016/j.jaridenv.2015.10.020, 2016.

443 Lyu S., Li Z., Zhang Y. and Wang X.: A 414-year tree-ring-based April–July minimum temperature reconstruction
444 and its implications for the extreme climate events, northeast China. *Clim. Past.* 12, 1879-1888, doi:10.5194/cp-12-
445 1879-2016, 2016.

446 Ma Z.G.: The interdecadal trend and shift of dry/wet over the central part of north China and their relationship to the
447 Pacific Decadal Oscillation (PDO). *Chin. Sci. Bull.*, 52(12), 2130-2139, 2007.

448 Mantua N., Hare S.: The Pacific decadal oscillation. *J. Oceanogr.* 58(1), 35-44, 2002.

449 Meehl G.A.: The annual cycle and interannual variability in the tropical Pacific and Indian Ocean regions. *Mon.*
450 *Weather. Rev.*, 115, 27-50, 1987.

451 Melvin T.M. and Briffa K.R.: A ‘signal-free’ approach to dendroclimatic standardisation. *Dendrochronologia*, 26,
452 71-86, doi: 10.1016/j.dendro.2007.12.001, 2008.

453 Nishimura M. and Yoshikawa I.: Nippon Kyokoshi Ko, Maruzen, Tokyo, an archival collection of disasters in
454 Japan, 1936 (in Japanese)

455 Ohayama M., Yonenobu H., Choi J.N., Park W.K., Hanzawa M. and Suzuki M.: Reconstruction of northeast Asia
456 spring temperature 1784-1990. *Clim. Past.*, 9, 261-266, doi:10.5194/cp-9-261-2013, 2013.

457 Omelko A., Ukhvatkina O. and Zmerenetsky A.: Disturbance history and natural regeneration of an old-growth
458 Korean pine-broadleaved forest in the Sikhote-Alin mountain range, Southeastern Russia. *For. Ecol. Manag.* 360,
459 221-234, doi: 10.1016/j.foreco.2015.10.036, 2016.

460 Omelko A.M. and Ukhvatkina, O.N.: Characteristics of gap-dynamics of conifer-broadleaved forest of Southern
461 Sikhote-Alin (Russia). *Plant World Asian Russ.*, 1, 106-113, 2012.

462 Popa I. and Bouriaud O.: Reconstruction of summer temperatures in Eastern Carpathian Mountain (Rodna Mts,
463 Romania) back to AD 1460 from tree-rings. *Int. J. Climatol.*, 34, 871-880, doi: 10.1002/joc.3730, 2014.

464 Porter T.J., Pisaric M.F., Kokelj S.V. and DeMontigny P.: A ring-width-based reconstruction of June-July minimum
465 temperatures since AD 1245 from white spruce stands in the Mackenzie Delta region, northwestern Canada.
466 *Quaternary. Res.*, 80, 167-179, doi: 10.1016/j.yqres.2013.05.004, 2013.

467 Raspopov OM, Dergachev VA, Esper J, Kozyreva OV, Frank D, Ogurtsov M, Kolström T, Shao X (2008) The
468 influence of the de Vries (~200-year) solar cycle on climate variations: Results from the Central Asian
469 Mountains and their global link. *Palaeogeogr Palaeoclimatol Palaeoecol* 259:6-16. doi:
470 10.1016/j.palaeo.2006.12.017

471 Raspopov O.M., Dergachev V.A., Kozyreva O.V., Kolström T., Lopatin E.V. and Luckman B.: Geography of 200-
472 year climate periodicity and Long-Term Variations of Solar activity. *Reg. Res. Russ.*, 2, 17-27, 2009.

473 Razzhigaeva N.G., Ganzei L.A., Mokhova L.M., Makarova T.R., Panichev A.M., Kudryavtseva E.P., Arslanov
474 Kh.A., Maksimov F.E. and Starikova A.A.: The Development of Landscapes of the Shkotovo Plateau of Sikhote-
475 Alin in the Late Holocene. *Reg. Res. Russ.*, 3, 65-80, doi:10.15356/0373-2444-2016-3-65-80, 2016.

476 Ren F. and Zhai P.: Study on Changes of China’s Extreme Temperatures During 1951–1990. *Sci. Atmos. Sin.*, 22,
477 217-227, 1998.

478 Sakaguchi Y.: Warm and cold stages in the past 7600 years in Japan and their global correlation. *Bull. Dep. Geogr.*
479 15, 1-31, 1983.

480 Shao X. and Wu X.: Reconstruction of climate change on Changbai Mountain, Northeast China using tree-ring data.
481 Quaternary. Sci., 1, 76-83, 1997.

482 Stokes M.A. and Smiley T.L.: Tree-ring dating. The University of Chicago Press, Chicago, London, 1968.

483 Tang H., Zhai P. and Wang Z.: On Change in Mean Maximum Temperature, Minimum Temperature and Diurnal
484 Range in China During 1951–2002. Climatic Environ Res., 10, 728-735, 2005.

485 Thapa U.K., Shan S.K., Gaire N.P. and Bhujju D.R.: Spring temperatures in the far-western Nepal Himalaya since
486 1640 reconstructed from *Picea smithiana* tree-ring widths. Clim dyn, 45(7), 2069-2081, doi: 10.1007/s00382-014-
487 2457-1, 2015.

488 Wang H., Shao X.M., Jiang Y., Fang X.Q. and Wu S.W.: The impacts of climate change on the radial growth of
489 *Pinus koraiensis* along elevations of Changbai Mountain in northeastern China. For. Ecol. Manag., 289, 333-340,
490 doi:10.1016/j.foreco.2012.10.023, 2013.

491 Wang X., Zhang M., Ji Y., Li Z., Li M. and Zhang Y.: Temperature signals in tree-ring width and divergent
492 growth of Korean pine response to recent climate warming in northeast Asia. Trees 31(2), 415-427, doi:
493 10.1007/s00468-015-1341-x, 2016.

494 Wang S., Liu J. and Zhou J.: The Climate of Little Ice Age Maximum in China. J. Lake. Sci., 15, 369-379, 2003.

495 Wang W., Zhang J., Dai G., Wang X., Han S., Zhang H. and Wang Y.: Variation of autumn temperature over the
496 past 240 years in Changbai Mountain of Northeast China: A reconstruction with tree-ring records. China. J. Ecol.,
497 31, 787-793, 2012.

498 Wang Z., Ding Y., He J. and Yu J.: An updating analysis of the climate change in China in recent 50 years. Ac
499 Meteorol Sin, 62, 228-236, 2004.

500 Wigley T.M.L., Briffa K.R. and Jones P.D.: On the average value of correlated time series, with applications in
501 dendroclimatology and hydrometeorology. J. Clim. Appl. Meteorol., 23, 201-213, 1984.

502 Wiles G.C., Solomina O., D'Arrigo R., Anchukaitis K.J., Gensiarovsky Y.V. and Wiesenberg N.: Reconstructed
503 summer temperatures over the last 400 year a based on larch ring widths: Sakhalin Island, Russian Far East. Clim.
504 Dyn., 45, 397-405, doi: 10.1007/s00382-014-2209-2, 2014.

505 Wilson R.J.S. and Luckman B.H.: Tree-ring reconstruction of maximum and minimum temperatures and the diurnal
506 temperature range in British Columbia, Canada. Dendrochronologia, 20, 1-12, 2002.

507 Wilson R.J.S., Luckman B.H.: Dendroclimatic reconstruction of maximum summer temperatures from upper
508 treeline sites in Interior British Columbia, Canada. Holocene, 13, 851-861, doi:10.1191/0959683603hl663rp, 2003.

509 Xie Z. and Cao H.: Asymmetric changes in maximum and mini- mum temperature in Beijing. Theor Appl Climatol,
510 55, 151-56, 1996.

511 Yin H., Guo P., Liu H., Huang L., Yu H., Guo S. and Wang F.: Reconstruction of the October mean temperature
512 since 1796 at Wuying from tree ring data. Adv. Clim. Change. Res., 5, 18-23, 2009.

513 Yin H., Liu H., Linderholm H.W. and Sun Y.: Tree ring density-based warm-season temperature reconstruction
514 since AD 1610 in the eastern Tibetan Plateau. Palaeogeogr, Palaeoclimatol, Palaeoecol, 426, 112-120, doi:
515 10.1016/j.palaeo.2015.03.003, 2015.

516 Young G.A.: Bootstrap: more than a stab in the dark. Statistical. Sci. 9, 382-415, 1994.

517 Zaiki M., Können G., Tsukahara T., Jones P., Mikami T. and Matsumoto K.: Recovery of nineteenth-century
518 Tokyo/Osaka meteorological data in Japan. Int J Climatol, 26, 399-423, doi:10.1002/joc.1253, 2006.

519 Zang C. and Biondi F.: Treeclim: an R package for the numerical calibration of proxy-climate relationships. Ecogr.
520 38, 001-006, doi: 10.1111/ecog.01335, 2015.

- 521 Zhang R.B., Yuan Y.J., Wei W.S., Gou X.H., Yu S.L., Shang H.M., Chen F., Zhang T.W. and Qin L.:
522 Dendroclimatic reconstruction of autumn-winter mean minimum temperature in the eastern Tibetan Plateau since
523 1600 AD. *Dendrochronologia*, 33, 1-7, doi: 10.1016/j.dendro.2014.09.001, 2015.
- 524 Zhao C., Ring G., Zhang Y., Wang Y.: Climate change of the Northeast China over the past 50 years. *J. Arid. Land.*
525 *Resour. Environ.*, 23, 25-30, 2009.
- 526 Zhu H.F., Fang X.Q., Shao X.M. and Yin Z.: Tree-ring-based February-April temperature reconstruction for
527 Changbai Mountain in Northeast China and its implication for East Asia winter monsoon. *Clim Past.*, 5, 661-666,
528 2009.
- 529 Zhu L., Li Z., Zhang Y. and Wang X.: A 211-year growing season temperature reconstruction using tree-ring width
530 in Zhangguangcai Mountains, Northeast China: linkages to the Pacific and Atlantic Oceans. *Int. J. Climatol.*, doi:
531 10.1002/joc.4906, 2016.
- 532 Zhu L., Li S., Wang X.: Tree-ring reconstruction of February-March mean minimum temperature back to 1790 AD
533 in Yichun, Northeast China. *Quaternary. Sci.*, 35, 1175-1184, doi: 10.11928/j.issn.1001-7410.2015.05.13, 2015.

534 **Tables and Figures**

535 **Table 1.** The sampling information and statistics of the signal-free chronology

	VUSr
Elevation (m a.s.l.)	700-900
Latitude (N), Longitude (E)	44°01'32'', E 134°13'15''
Core (live trees) / sample (dead trees)	25/20
Time period / length (year)	1451-2014 / 563
MS	0.253
SD	0.387
AC1	0.601
R	0.691
EPS	0.952
Period with EPS>0.85 / length (year)	1602-2014 / 412
Period with EPS>0.75 / length (year)	1529-2014 / 485
Skew/Kurtosis	0.982/5.204

536 MS – mean sensitivity, SD – standard deviation, AC1 – first-order autocorrelation, EPS – expressed population signal

537

538 **Table 2.** Calibration and verification statistics of the reconstruction equation for the common period 1971-2003 of

539 **Bootstrap**

Statistical item	Calibration	Verification (Bootstrap, 199 iterations)
r	0.62	0.62 (0.54-0.70)
R ²	0.39	0.39 (0.27-0.41)
R ² _{adj}	0.36	0.37 (0.37-0.40)
Standard error of estimate	1.20	1.11
F	18.76	18.54
P	0.0001	0.0001
Durbin-Watson	1.73	1.80

540

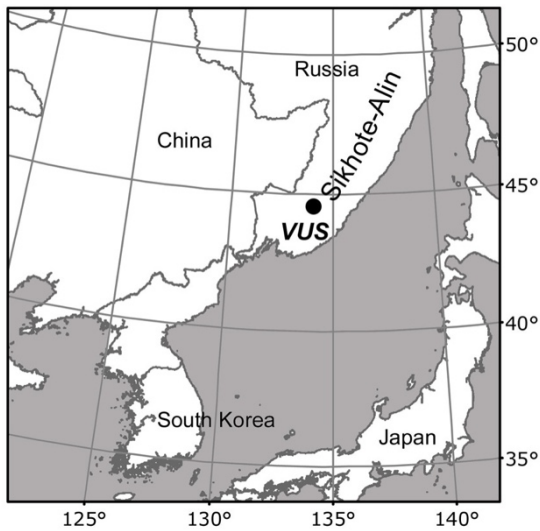
541 **Table 3.** Cold and warm periods based on the results of this study compared with other researches

Period	Southern Sikhote-Alin (this study)	Laobai Mountain (Lyu et al., 2016)	Changbai Mountain (Zhu et al., 2009)
Cold	1538-1544; 1549-1554	*	*
	—	1605-1616	
	1643-1649; 1659-1667	1645-1677	*
	1675-1689	1684-1691	*
	1791-1801; 1807-1818	—	1784-1815
	1822-1827; 1836-1852		1827-1851
	1868-1887	—	1878-1889
	1911-1925	1911-1924; 1930-1942; 1951-1969	1911-1945
Warm	1561-1584	*	*

1603-1607; 1614-1618	—	*
1738-1743	—	—
1756-1759; 1776-1781	1767-1785	1750-1783
<i>1787-1793**</i>	1787-1793	—
<i>1795-1807**</i>	1795-1807	—
<i>1855-1865**</i>	—	1855-1877
1944-2014	1991-2008	1969-2009

542 Note: *italic *** – the periods which agreement with VUSr but not reliably for VUSr; * - the reconstruction not
543 covering this period.

544



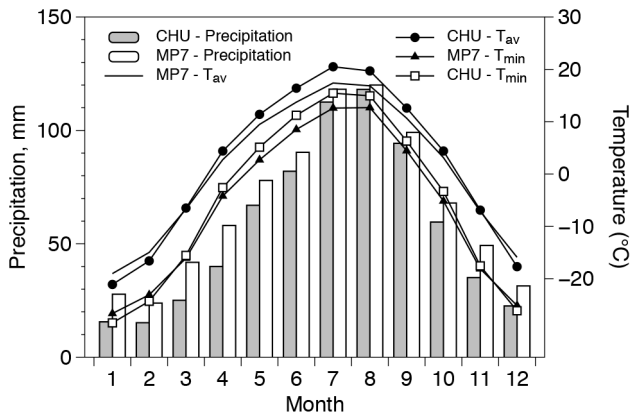
545

546

Figure 1: Location of the study area on the Sikhote-Alin Mountains, Southeastern Russia. VUS is Verkhneussyriysky

547

Research Station



548

549

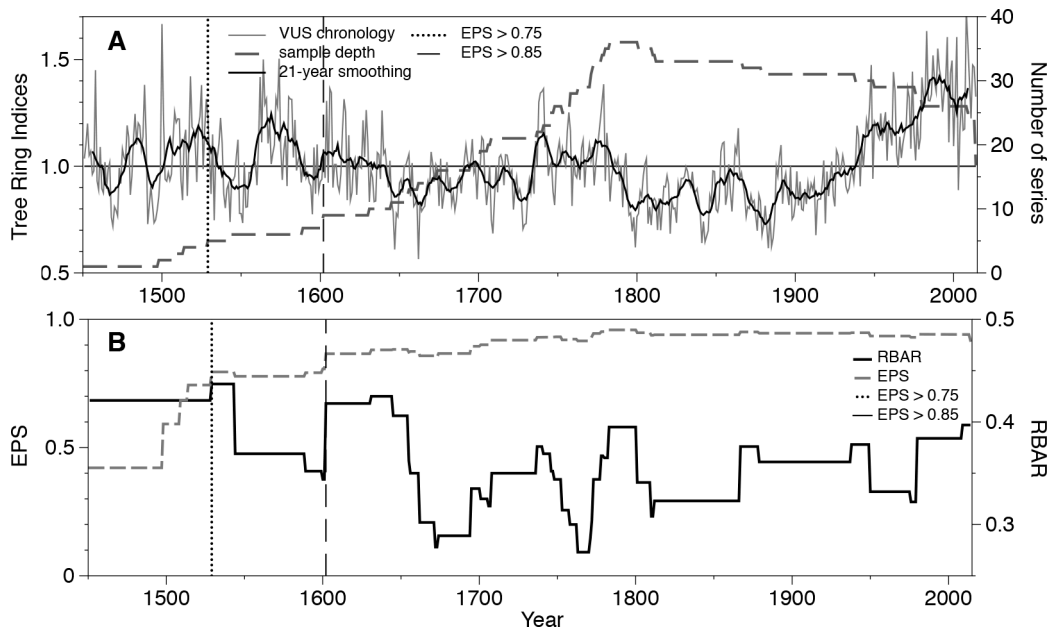
Figure 2: Mean monthly (1936-2004), minimum temperature (1971-2003) and total precipitation (1936-2004) at

550

Chuguevka and mean monthly, minimum temperature and total precipitation for VUS meteorological station (MP7)

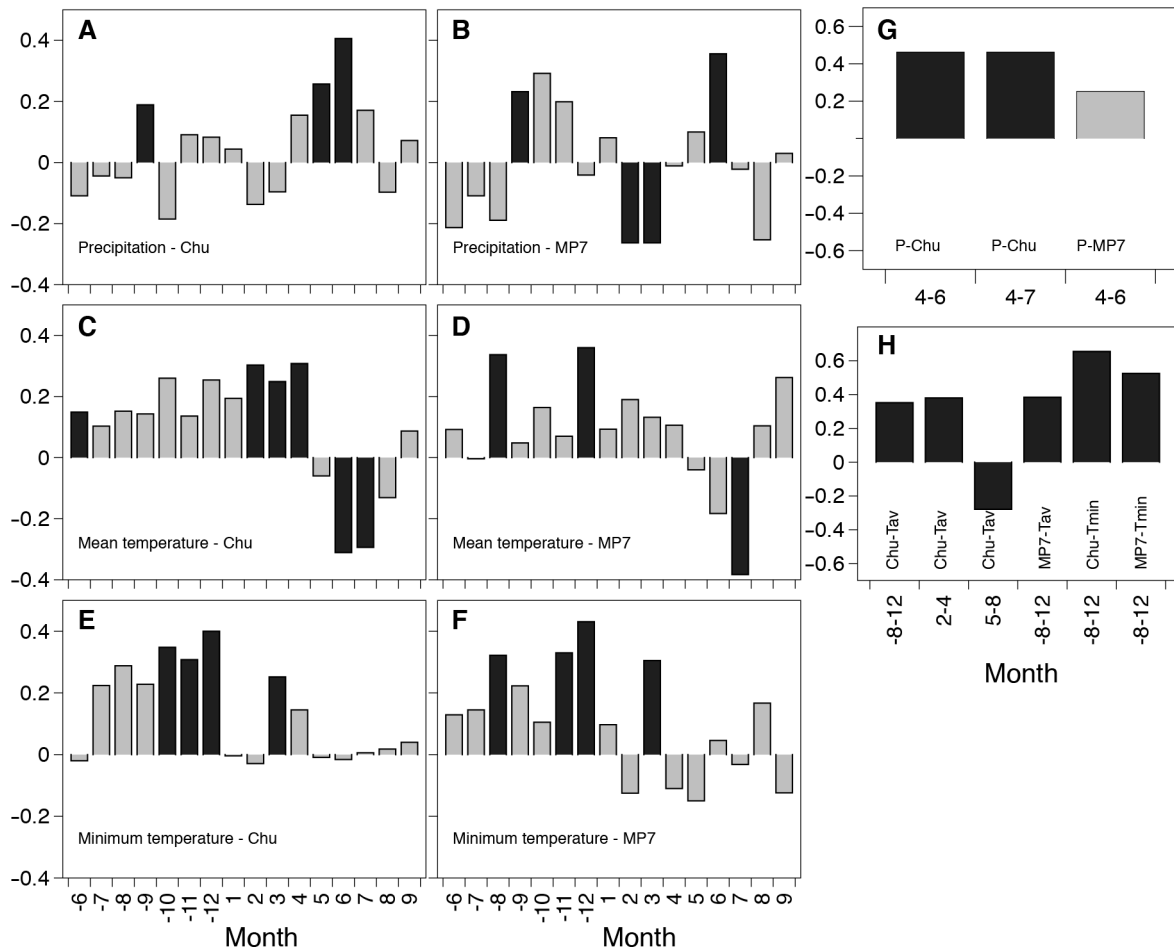
551

(1966-2000)



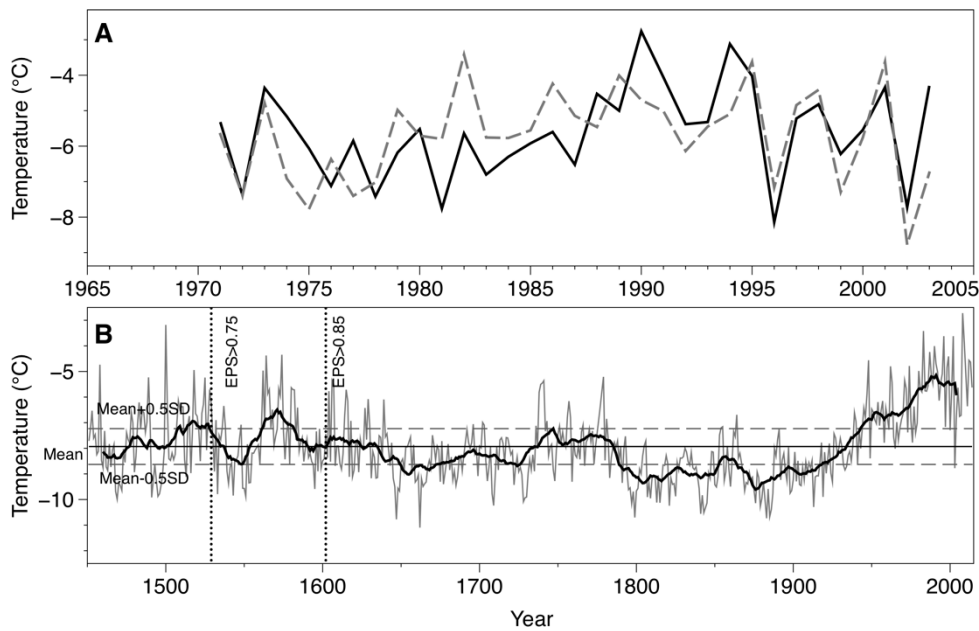
552
553
554

Figure 3: Variations of the VUS chronology and sample depth (a) and the expressed population signal (EPS) and average correlation between all series (Rbar) VUS chronology from AD 1451 to 2014 (b)



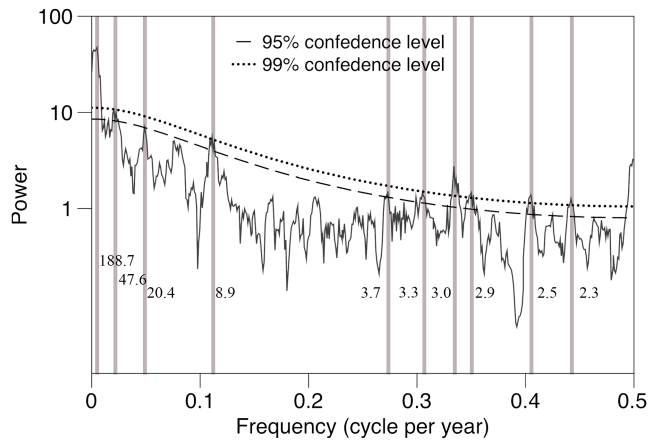
555
556
557
558
559
560

Figure 4: Correlations between the monthly mean meteorological data and VUS chronology
A, C, E – Chuguevka (Chu) and VUS chronology; B, D, F - VUS meteorological station (MP7) and VUS chronology;
G – correlation coefficients between VUS chronology and the precipitation of different month combinations; H –
correlation coefficients between VUS chronology and the temperature of different month combinations. The black
bars are significant value.



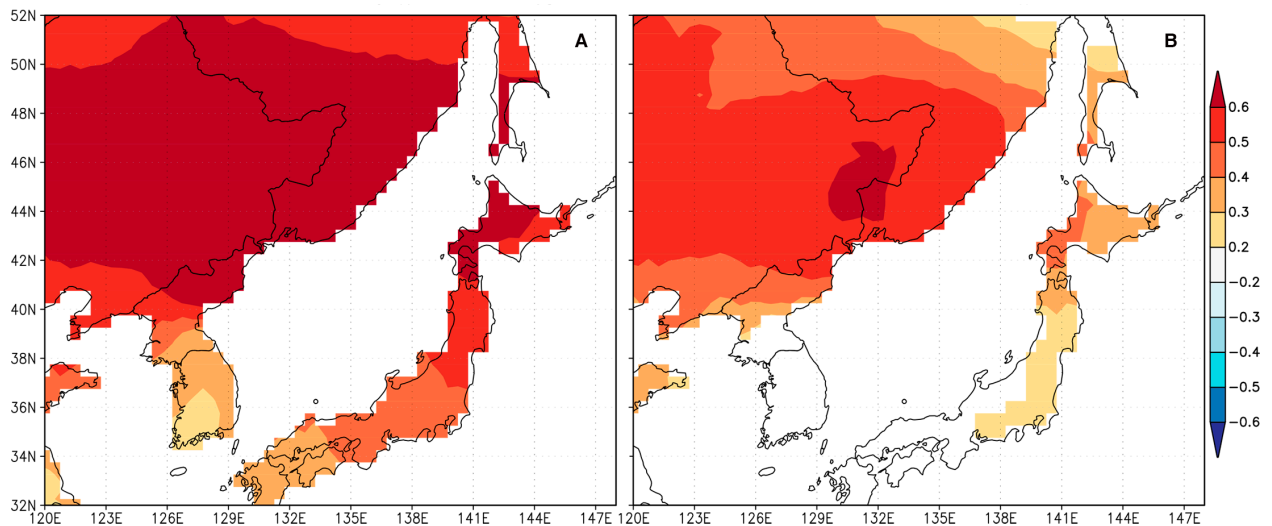
561
562
563
564

Figure 5: (a) Actual (black line) and reconstructed (dash line) August – December minimum temperature for the common period of 1971-2003; (b) reconstruction of August – December minimum temperature (VUSr) to Southern part of Sikhote-Alin for the last 563 years. The smoothed line indicates the 21-year moving average.



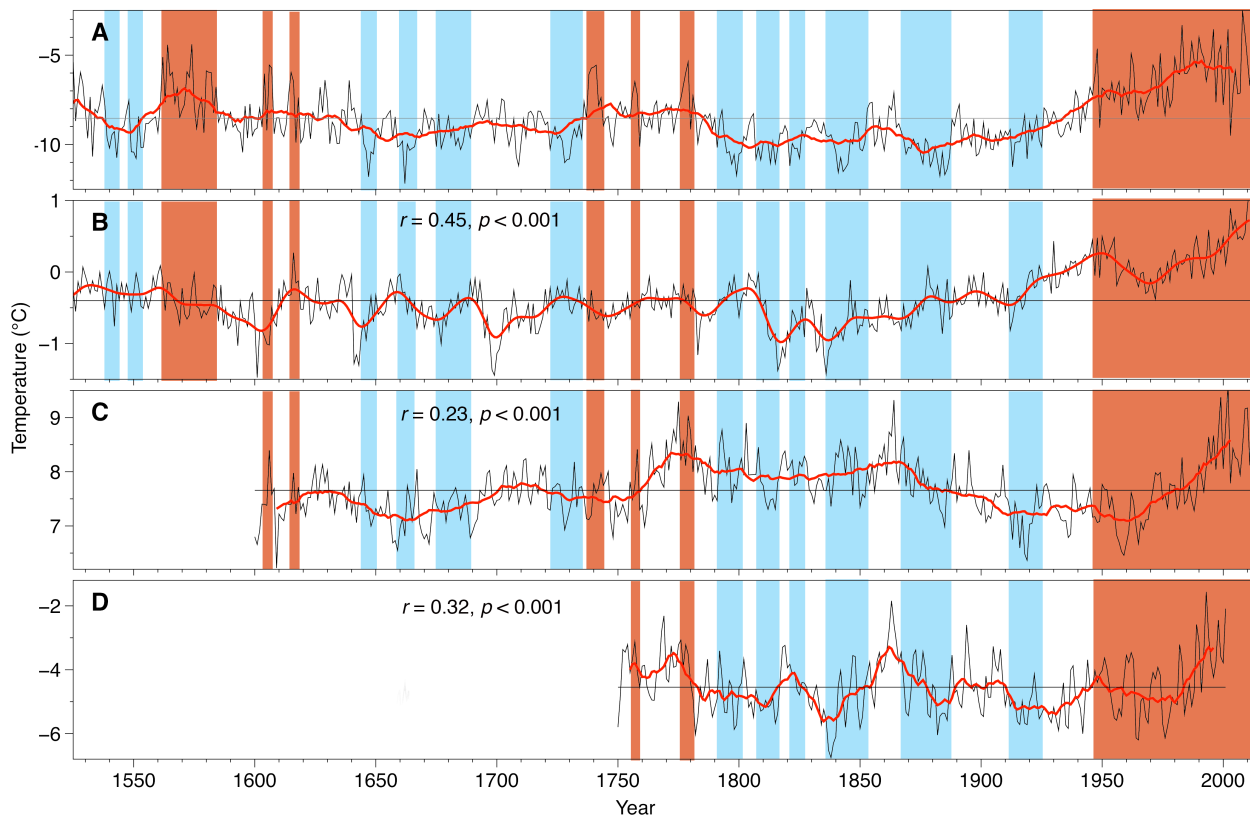
565
566
567

Figure 6: The MTM power spectrum of the reconstructed August – December minimum temperature (VUSr) from 1529 to 2014



568

569 **Figure 7:** Spatial correlations between the observed (a) and reconstructed (b) August – December minimum
 570 temperature (VUS) in this study and regional gridded annual minimum temperature from CRU TS 4.00 over their
 571 common period 1960–2003 ($p < 10\%$)
 572



573
 574 **Figure 8:** (a) August-December mean minimum temperature reconstructed (VUSr) on southern part of Sikhote-
 575 Alin, (b) Northern Hemisphere extratropical temperature (Willes et al., 2016), (c) April – July minimum temperature
 576 on Laobai Mountain by Lyu et al., 2016, and (d) February – April temperature established by Zhu et al. (2009) on
 577 Changbai Mountain. Black lines denote temperature reconstruction values, and red color lines indicate the 21-year
 578 moving average; red and blue fields – warm and cold period consequently (in this study)